Noname manuscript No.
(will be inserted by the editor)

Formation Control and Obstacle/Collision Avoidance with Dynamic Constraints

Shaoyang Mu · Pingfang Zhou

Received: date / Accepted: date

Abstract This paper studies the leader-follower formation control problem of unmanned air vehicles(UAVs) flying with dynamic constraints in an obstacle-laden environment. Firstly, formation protocols are presented for UAV swarm systems. Necessary and sufficient conditions for UAV swarm systems to achieve formations are presented based on graph theory. A formation tracking protocol is designed to drive the followers to track the leader. Then, an improved obstacles avoidance method based on potential field method is designed by combining with local rules considering dynamic constraints. The improved method can avoid potential field falling into local minimum and have good global searching ability. The stability of the presented approach is proved by using Lyapunov stability theory. Finally, numerical simulations are presented to demonstrate the effectiveness of the designed approach.

Keywords Leader-follower formation · consensus algorithm · potential filed · collision avoidance

1 Introduction

Cooperative control problems of multiagent systems have attracted a lot of attention in recent years [1]-[2]. This is partly due to its broad applications in flocking, formation control and robot target tracking [3]-[8].

Typical approaches for formation control include leader-follower, behavioral, virtual structure/virtual leader approaches. Some papers [9]-[10] discuss the leader-follower approach.In these papers, the first vehicle is regarded as

Shaoyang Mu
School of Aeronautics and Astronautics,Shanghai Jiao Tong University
E-mail: shaoyangmu@sjtu.edu.cn

Pingfang Zhou
School of Aeronautics and Astronautics,Shanghai Jiao Tong University
E-mail: zhoupf@sjtu.edu.cn

the leader and others are regarded as followers. The leader vehicle flies according to the pre-planned trajectory, the follower vehicles follow the leader's motion, maintaining a desired geometric structure. The leader-follower approach simplifies the control of multiagent systems. However, if the leader is out of control, the formation will not be maintained. The behavioral approach is introduced by papers [11]-[12]. The main content of this approach is to design various basic behaviors, obstacle/collision avoidance, target searching and formation maintaining, i.e. The behavioral approach is a fully distributed control structure with real-time feedback characteristics and has better flexibility. However, it's difficult to carry out mathematical analysis and corresponding stability analysis of the system. These papers [13]-[15] discuss the approach of virtual structure/virtual leader. The entire formation is designed as a single rigid virtual structure and each vehicle is a fixed point. During the formation flying, each vehicle only needs to track the fixed point motion corresponding to the rigid structure, The virtual structure/virtual leader approach simplifies task description and assignment. However, it's a centralized control approach with poor reliability.

Consensus problems are important and challenging research topics in multiagent coordination. The basic idea of consensus is that a group of agents reach an agreement on their common states via local interaction. In [16], the author has proved that most approaches of leader-follower, behavioral, virtual structure/virtual leader can be regarded as special cases of consensus-based approaches. And the weakness of the previous approaches can be overcome. In the past decade, consensus algorithms have been studied in various multiagent systems [17]-[25]. In [17], the formation control protocol is designed to guarantee the consistency of vehicles in altitude. In [18], considering the input constraints, a non-linear centrally-free consistency algorithm is used to achieve altitude maintaining of multi-UAV systems. In [18]-[20], consensus algorithm takes the form of first-order dynamics is used, and in [21]-[23], the authors extend it to second-order dynamics under undirected information flow. In [24], the consensus problem of multiagent systems with switching topologies is discussed, a formation protocol is designed to solve the average consensus problem. In [25], a formation control problem with time-varying is discussed under the case of a spanning tree in the network topology. The stability conditions are obtained and the experimental verification is carried out.

Most of the aforementioned work haven't taken collision/obstacle avoidance into consideration, but collision would occur while the UAVs are flying in formation. Note that in [26] and [27], the artificial potential field approach is used to achieve collision/obstacle avoidance. Attractive potential fields are assigned to target points and repulsive potential are assigned to obstacles. The vehicles move along the direction under resultant forces and toward the attractive target point. However, the weakness of the artificial potential field approach is that it's easy to fall into local minimum. What's more, vehicles have dynamic constraints, maximum turning angle and maxi climb angle, etc.

In this paper, we study the consensus problem of second-order continuous-time UAVs system. Graph theory is used to describe network topology of the

system. A consensus algorithm to achieve formation control is presented. The stability conditions of the consensus algorithm are analyzed by using a Lyapunov function and LaSalle's principle. Contributions of this paper include using a consensus algorithm to achieve formation control and taking collision/obstacle avoidance into consideration compared with the second-order consensus algorithm studied in [22]. Compared with [26], considering dynamic constraints, an improved artificial potential field based approach with dynamic constraints is designed to achieve collision/obstacle avoidance. Our method can avoid potential field function falling into a local minimum and improve the global searching ability.

In Section II, some basic concepts and results about graph theory and the system model are introduced. In Section III, a formation protocol is presented and stability conditions are analyzed. In Section IV, simulation results of formation control, collision/obstacle avoidance in 2-D are shown. Conclusions and future work are discussed in Section V.

2 PRELIMINARIES AND SYSTEM MODEL

2.1 Notations

R_n denotes the set of all n dimensional real column vectors.
1_n and 0_n denote the $n \times 1$ column vector of all-one and all-zero, respectively.
$\boldsymbol{I}_n$ and $\boldsymbol{0}_{(n\times n)}$ denote the identity matrix and zero matrix with dimension n, respectively.
For a given $\lambda \in C$, $Re(\lambda)$ and $Im(\lambda)$ denote the real part and the imaginary part of λ, respectively.
Let $\otimes$ denote the Kronecker product.
$\| \boldsymbol{A} \|$ denotes the norm of the matrix/vector $\boldsymbol{A}$.

2.2 Graph Theory

Here, we introduce some definitions and results about graph theory(for more details, please refer to [28]).

An undirected graph $G = (V, E, \boldsymbol{A})$ is used to describe the communication among n agents. $V = s_1, s_2, \cdots, s_n$ is the set of nodes. $E = (s_i, s_j) \in s \times s, i \neq j$ is the set of edges. An edge of G is denoted by $s_{ij} = (s_i, s_j)$, if $s_i \in E \longleftrightarrow s_{ji} \in E$, the graph is said to be undirected graph. $\boldsymbol{A} = [a_{ij}]$ is a weighted adjacency matrix with $a_{ii} = 0, a_{ij} = a_{ji} \geq 0$, where $a_{ij} > 0$ if and only if $s_{ij} \in E$. $N_i = s_j \in V : (s_i, s_j) \in E$ denotes the set of neighbors of node s_i. The Laplacian matrix of undirected graph is defined as $\boldsymbol{L} = [l_{ij}]$, where $l_{ij} = \sum_{j=1}^{n} a_{ij}$ and $l_{ij} = -a_{ji}, i \neq j$. If there is a path from any node to each other node, the graph is considered as connected. Assuming that a collection of graphs $\overline{G}_1, \overline{G}_2, \cdots, \overline{G}_m$ with the same node set V is defined as the graph $\overline{G}_{1\sim m}$. The node set is V and the edge set $\overline{G}_{1\sim m}$ is the union of the edge sets of all graphs

in the collection. Besides, if the graph $\overline{G}_{1\sim m}$ is connected , the collection of graphs $\overline{G}_1, \overline{G}_2, \cdots, \overline{G}_m$ will be considered as jointly-connected.

Lemma 1 *[21]: $\boldsymbol{L}$ is the matrix of an undirected graph, then $\boldsymbol{L}$ has a simple zero eigenvalue and $\boldsymbol{1}_n$ is the associated eigenvector, that means, $\boldsymbol{L}\boldsymbol{1}_n = 0$.*

2.3 System Dynamics and Control Protocol

In order to focus on studying formation control law, an individual UAV is modeled as a point-mass system. The consensus problem for second-order multiagent systems in 2-D plane is considered. The dynamics of each UAV can be described as a double integrator as [16], [21]

$$\begin{cases} \dot{\xi}_i(t) = \zeta_i(t) \\ \dot{\zeta}_i(t) = \boldsymbol{u}_i(t) \end{cases} \tag{1}$$

Where $i = 1, 2, \cdots, N$, $\xi_i(t) = x = [x_i, y_i]^T \in R^n$ and $\zeta_i(t) = v = [v_{xi}cos\theta_i, v_{yi}sin\theta_i]^T \in R^n$ denote the position state and velocity state of UAV i, respectively. θ_i and $u_i(t) \in R^n$ denote the heading angle and control input, respectively. If the control protocol can guarantee that the state of all UAVs reach $[\xi_j(t) \to \xi_i(t)] \to \boldsymbol{r}_{ij}$ and $[\zeta_j(t) \to \zeta_i(t)] \to \zeta^*$ as $t \to \infty$ for all UAVs from $1, 2, \cdots, N$, then, we can say the formation is achieved with desired speed ζ^*. Where $\boldsymbol{r}_{ij}$ denotes the desired distance difference between UAV i and j, ζ^* denotes the desired speed.

In [22], the consensus protocol is proposed to solve the formation control without considering dynamic constraints and collision/obstacle avoidance. In this paper, our main objective is to extend the work of [22] to solve the consensus problem with jointly-connected topologies and collision/obstacle avoidance. Here, we presented the following linear consensus protocol

$$\boldsymbol{u}_i(t) = \sum_{V_j \in N_i(t)} a_{ij}\{k_1[\xi_j(t) - \xi_i(t) - \boldsymbol{r}_{ij}] + k_2[\zeta_j(t) - \zeta_i(t)]\} - k_3(\zeta_i - \zeta^*) \tag{2}$$

Where a_{ij} denotes the element of the weighted adjacency matrix, $N_i(t)$ denotes the set of neighbors of node s_i and the value of k_1, k_2, k_3 all are positive .

3 Formation Control Protocol Design And Analysis

3.1 Formation Control Protocol Design

In order to analysis the performance of formation control protocol, we give the concept of formation center, which is the center of formation structure. For example, as is shown in Fig. 1, assume that the formation structure is a regular triangle. Where O denotes the origin of Cartesian coordinate system,

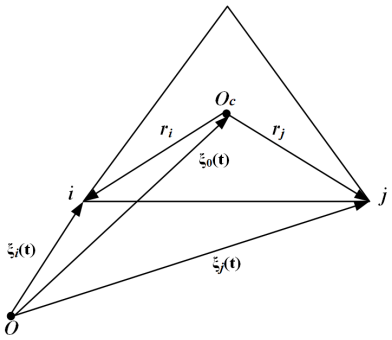

Fig. 1: Formation Plane

O_C denotes the formation center, $\xi_i(t), \xi_j(t), \xi_0(t)$denote the position state of UAV and formation center, respectively, $\boldsymbol{r}_i, \boldsymbol{r}_j$ denote the distance from formation center to UAV i, j, respectively.

Then, consensus protocol (2) can be transformed into

$$\boldsymbol{u}_i(t) = \sum_{V_j \in N_i(t)} a_{ij}\{k_1[(\xi_j(t) - \boldsymbol{r}_j) - (\xi_i(t) - \boldsymbol{r}_i)] + k_2[\zeta_j(t) - \zeta_i(t)]\} - k_3(\zeta_i - \zeta^*) \tag{3}$$

Where $\boldsymbol{r}_{ji} = \boldsymbol{r}_j - \boldsymbol{r}_i$. In the next, the consensus protocol (3) will be extended to achieve formation control.

3.2 Potential Forces

According to the potential field method in [22], the potential forces will be designed to achieve collision/obstacle avoidance as following.

3.2.1 Attractive Potential Fields of Target

The position state of UAV i is denoted as $\xi_i = [x_i, y_i]^T \in R^2$. The target applies attractive force to UAV and the value of the force is in reverse proportion to the distance from UAV to target. The attractive potential field $U_{att}(\xi_i, \xi_G)$ is denoted as

$$U_{att}(\xi_i, \xi_G) = 0.5\varepsilon d^2(\xi_i, \xi_G) \tag{4}$$

Where $\varepsilon > 0$, denotes the gain coefficient of attractive potential field, $\xi_G = [x_g, y_g]^T \in R^2$ denotes the position state of target $G, d(\xi_i, \xi_G)$ denotes the distance from UAV i to target G and the attractive force $\boldsymbol{F}_{att}(\xi_i, \xi_G)$ is denoted as

$$\boldsymbol{F}_{att}(\xi_i, \xi_j) = -\nabla U_{att}(\xi_i, \xi_j) = -\varepsilon(\xi_i - \xi_G) \tag{5}$$

3.2.2 Repulsive Potential Fields of Obstacle

The obstacles expert repulsive force to UAV and the value of the force is in reverse proportion to the distance from UAV to target. The repulsive potential field $U_{rep}(\xi_i, \xi_{obs})$ is denoted as

$$U_{rep}(\xi_i, \xi_{obs}) = \begin{cases} 0.5\eta(\frac{1}{d(\xi_i,\xi_{obs})} - \frac{1}{d_0})^2 d^n(\xi_i, \xi_G) & , d(\xi_i, \xi_{obs}) \leq 0 \\ 0 & , d(\xi_i, \xi_{obs}) > d_0 \end{cases} \tag{6}$$

Where $\eta > 0$ denotes the gain coefficient of repulsive potential field, $d(\xi_i, \xi_{obs})$ denotes the distance from UAV i to obstacles. d_0 denotes the affects distance of obstacle. d_0 is generally chosen as $d_0 \leq min(d_1, d_2)$ in order to avoid repulsive potential field falling into local minimum, where d_1 represents half of the smallest distance between obstacles, d_2 represents the minimum distance from target to each obstacle. In order to operate the UAV more flexible, d_0 can be chosen dynamically according to the speed of UAV.

$$d_0 = d_0^{min} + k_0 v \tag{7}$$

Where d_0^{min} denotes the minimum distance to avoid obstacle, k_0 is associated with the performance of UAV.

The repulsive force is denoted as $\boldsymbol{F}_{rep}(\xi_i, \xi_{obs}) = -\nabla_{\xi_i} U_{rep}(\xi_i, \xi_{obs})$

$$\boldsymbol{F}_{rep}(\xi_i, \xi_{obs}) = \begin{cases} \boldsymbol{F}_{rep1}\boldsymbol{n}_{ov} + \boldsymbol{F}_{rep2}\boldsymbol{n}_{vG} & , d(\xi_i, \xi_{obs}) \leq d_0 \\ 0 & , d(\xi_i, \xi_{obs}) > d_0 \end{cases} \tag{8}$$

Where $\boldsymbol{n}_{ov}$ and $\boldsymbol{n}_{vG}$ denote unit vectors with the direction from obstacle to UAVs and from UAVs to target.

$$\boldsymbol{F}_{rep1} = \eta(\frac{1}{d(\xi_i, \xi_{obs})} - \frac{1}{d_0})\frac{d^n(\xi_i, \xi_G)}{d^2(\xi_i, \xi_{obs})} \tag{9}$$

$$\boldsymbol{F}_{rep2} = 0.5n\eta(\frac{1}{d(\xi_i, \xi_{obs})} - \frac{1}{d_0})d^{n-1}(\xi_i, \xi_G) \tag{10}$$

3.2.3 Collision avoidance potential field of UAVs

In this paper, obstacle avoidance method is used to achieve collision avoidance. For UAV i, the other UAVs all are obstacles. The other UAVs expert repulsive forces to UAV i. The collision avoidance potential field is denoted as

$$U_{rep}(\xi_i, \xi_j) = \begin{cases} 0.5k(\frac{1}{d(\xi_i,\xi_j)} - \frac{1}{d_{safe}})^2 & , d(\xi_i, \xi_j) \leq d_{safe} \\ 0, & , d(\xi_i, \xi_j) > d_{safe} \end{cases} \tag{11}$$

Where $k > 0$ denotes the gain coefficient of collision avoidance potential field, $d(\xi_i, \xi_j)$ denotes the distance between UAV i and j, d_{safe} denotes the

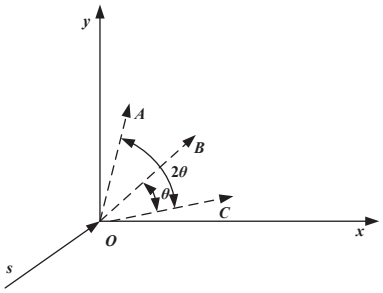

Fig. 2: The range of motion

safety distance of each UAV. The repulsive force between UAV i and j is denoted as $\boldsymbol{F}_{ij} = -\nabla U_{rep}(\xi_i, \xi_j)$.

$$\boldsymbol{F}_{ij} = \begin{cases} k(\frac{1}{d(\xi_i,\xi_j)} - \frac{1}{d_{safe}})^2 \frac{1}{d^2(\xi_i,\xi_j)} \boldsymbol{n}_{ij} & , d(\xi_i, \xi_j) \leq d_{safe} \\ 0 & , d(\xi_i, \xi_j) > d_{safe} \end{cases} \tag{12}$$

Where $\boldsymbol{n}_{ij}$ is a unit vector with the direction from UAV j to i. Noted that the value of $\boldsymbol{F}_{ij}$ is associated with safety distance d_{safe}. Then, the total forces $\boldsymbol{F}_{ij}^{all}$ of UAV i is denoted as

$$\boldsymbol{F}_{ij}^{all} = \begin{cases} \sum_{j=1}^{n} \boldsymbol{F}_{ij} & , d(\xi_i, \xi_j) \leq d_{safe} \\ 0 & , d(\xi_i, \xi_j) > d_{safe} \end{cases} \tag{13}$$

3.3 Dynamic Constraints

As in [30], we take velocity constraints into consideration. The velocity v is associated with heading angle, $v = [v_{xi}\cos(\theta_i),\ v_{yi}\sin(\theta_i)]^T \in R^n$, and the heading angle is related to resultant force. However, due to the performance constraints of UAVs, the motion direction of UAVs can't be completely determined by the calculated resultant force in each step. Heading angle should be corrected after calculating resultant force in each step. As shown in Fig. 2, assume that node s and flight direction of UAV i at current are known. $\angle\ \boldsymbol{COB}$ denotes the maximum heading angle θ. Therefore, the next motion direction of UAV i is limited to $\angle \boldsymbol{AOB} = 2\theta$.

If the direction of resultant force is under the range of 2θ, motion direction of UAV i will be the direction of resultant force. Otherwise, it should be corrected. The corrected heading angle is represented as

$$\theta_0 = \begin{cases} \theta & , \theta_{real} > \theta \\ \theta_{real} & , |\theta_{real}| < \theta \\ -\theta & , \theta_{real} < -\theta \end{cases} \tag{14}$$

Where θ_{real} denotes the direction angle of resultant force, and θ_0 denotes the heading angle of UAV in next step after being corrected. The positive

heading angle is counterclockwise. By limiting heading angle, the velocity constraints is achieved.

Remark 1: Agents are subject to bounded maximum linear velocity because of dynamic limitations and most of the agents are subject to the positive-minimum velocity in case of stall conditions. In 3-D plane, it should be pointed out that pitch angle also should be taken into account.

3.4 Collision/Obstacle Avoidance Protocol Design

Based on the theory introduced above and the protocol (3), here, collision/obstacle avoidance protocol for UAV i is designed as

$$\begin{aligned}\boldsymbol{u}_i(t) = k_1 \sum_{s_j \in N_i(t)} a_{ij}(t)[\xi_j(t) - \xi_i(t) - \boldsymbol{r}_{ij}] + k_2 \sum_{obs=1}^{l} \boldsymbol{F}_{rep}(\xi_i, \xi_{obs} + k_3 \boldsymbol{F}_{att}(\xi_i, \xi_G) \\ + k_4 \sum_{s_j \in \overline{N}_i(t)} \boldsymbol{F}_{ij} - \zeta_i(t) + v_0\end{aligned} \tag{15}$$

Where k_1, k_2, k_3, k_4 all are positive number, $a_{ij}(t)$ denotes the weighted adjacency of communication topology G, $N_i(t)$ denotes the set of neighbors of UAV $i, \overline{N}_i(t)$ denotes the set of collision neighbors of UAV i, l denotes the number of obstacles currently detected by UAV i.

Remark 2: The Variable-weight method is used to make the protocol (15) more widely applied in practice, which means, (a): if the obstacle is not detected, $k_1, k_3 > k_2 = 0$, (b): if the obstacle is detected,$k_2 > k_1, k_3 > 0$. Substituting (4),(8),(12) into (15), then protocol (15) can be rewritten as

$$\begin{aligned}\boldsymbol{u}_i(t) = k_1 \sum_{s_j \in N_i(t)} a_{ij}(t)[\xi_j(t) - \xi_i(t) - \boldsymbol{r}_{ij}] - k_2 \sum_{obs=1}^{l} \nabla_{\xi_i} U_{rep}(\xi_i, \xi_{obs}) \\ - k_3 \nabla_{\xi_i} U_{att}(\xi_i, \xi_G) - k_4 \sum_{s_j \in \overline{N}_i(t)} \nabla_{\xi_i} U_{rep}(\xi_i, \xi_j) - \zeta_i(t) + \boldsymbol{v}_0\end{aligned} \tag{16}$$

According to the concept of formation center in Section II, (16) can be rewritten as

$$\begin{aligned}\boldsymbol{u}_i(t) = k_1 \sum_{s_j \in N_i(t)} a_{ij}(t)[(\xi_j(t) - \boldsymbol{r}_j) - (\xi_i(t) - \boldsymbol{r}_i)] - k_2 \sum_{obs=1}^{l} \nabla_{\xi_i} U_{rep}(\xi_i, \xi_{obs}) \\ - k_3 \nabla_{\xi_i} U_{att}(\xi_i, \xi_G) - k_4 \sum_{s_j \in \overline{N}_i(t)} \nabla_{\xi_i} U_{rep}(\xi_i, \xi_j) - \zeta_i(t) + \boldsymbol{v}_0\end{aligned} \tag{17}$$

Where $\boldsymbol{r}_{ji} = \boldsymbol{r}_j - \boldsymbol{r}_i$. Let $\hat{\xi}_i(t) = \xi_i(t) - \xi_0(t) - \boldsymbol{r}_i, \hat{\zeta}_i(t)\zeta_i(t) - \boldsymbol{v}_0(t)$, then, (17) can be transformed into

$$\begin{aligned}\boldsymbol{u}_i(t) = k_1 \sum_{s_j \in N_i(t)} a_{ij}(t)[\hat{\xi}_j(t) - \hat{\xi}_i(t)] - k_2 \sum_{obs=1}^{l} \nabla_{\xi_i} U_{rep}(\hat{\xi}_i + \xi_0 + \boldsymbol{r}_i, \xi_{obs}) \\ - k_3 \nabla_{\xi_i} U_{att}(\hat{\xi}_i + \xi_0 + \boldsymbol{r}_i, \xi_G) - k_4 \sum_{s_j \in \overline{N}_i(t)} \nabla_{\xi_i} U_{rep}(\hat{\xi}_i, \hat{\xi}_j) - \hat{\zeta}_i\end{aligned} \tag{18}$$

By protocol (18), then, swarm system (1) can be rewritten as

$$\begin{cases} \dot{\hat{\xi}}_i(t) = \hat{\zeta}_i(t) \\ \dot{\hat{\xi}}_i(t) = k_1 \sum_{s_j \in N_i(t)} a_{ij}(t)[\hat{\xi}_j(t) - \hat{\xi}_i(t)] - k_2 \sum_{obs=1}^{l} \nabla_{\xi_i} U_{rep}(\hat{\xi}_i + \xi_0 + \boldsymbol{r}_i, \xi_{obs}) \\ \qquad -k_3 \nabla_{\xi_i} U_{att}(\hat{\xi}_i + \xi_0 + \boldsymbol{r}_i, \xi_G) - k_4 \sum_{s_j \in \overline{N}_i(t)} \nabla_{\xi_i} U_{rep}(\hat{\xi}_i, \hat{\xi}_j) - \hat{\zeta}_i \end{cases} \tag{19}$$

In the next, the stability of the system will be analyzed.

3.5 Formation Analysis

Lemma 2 *:Considering a UAV system with n agents and the communication topology is jointly connected. Assume that the number of obstacles ξ_{obs} is l (obs $= 1, 2, \cdots, l$) and the total energy V_t of UAV system is a finite value during the flight, that is, $V_t \leq V_0$. Then, under protocol* (16)*, the desired formation is achieved, that is, $\xi_j(t) - \xi_i(t) = \boldsymbol{r}_{ij}$.*

Proof: Here, we present the following Lyapunov candidate function V.

$$\begin{aligned} V = \sum_{i=1}^{n} [\frac{1}{2} k_4 \sum_{s_j \in \overline{N}_i(t)} U_{rep}^{ij} + k_2 \sum_{obs=1}^{l} U_{rep}^{i}(\hat{\xi}_i + \xi_0 + \boldsymbol{r}_i, \xi_{obs}) + \frac{1}{2} \hat{\zeta}_i^T \hat{\zeta}_i \\ + \frac{k_1}{4} \sum_{s_j \in N_i(t)} a_{ij}(\hat{\xi}_i - \hat{\xi}_j)^2 + k_3 U_{att}^{i}(\hat{\xi}_i + \xi_0 + \boldsymbol{r}_i, \xi_G)] \end{aligned} \tag{20}$$

Clearly, we can see that V is a semidefinite function. Substituting (19) into (20), the time derivative of function V is given by

$$\begin{aligned}\dot{V} = \sum_{i=1}^{n}[k_4\hat{\zeta}_i^T \sum_{s_j\in\overline{N}_i(t)} \nabla_{\xi_i} U_{rep}(\hat{\xi}_i,\hat{\xi}_j) + k_2 \sum_{obs=1}^{l} \nabla_{\xi_i} U_{rep}(\hat{\xi}_i+\xi_0+\mathbf{r}_i,\xi_{obs}) \\ + k_3\nabla_{\xi_i} U_{att}(\hat{\xi}_i+\xi_0+\boldsymbol{r}_i,\xi_G) + \hat{\zeta}_i^T k_1 \sum_{s_j\in N_i(t)} a_{ij}(t)[\hat{\xi}_j(t)-\hat{\xi}_i(t)] \\ - k_2\hat{\zeta}_i^T k_2 \sum_{obs=1}^{l} \nabla_{\xi_i} U_{rep}(\hat{\xi}_i+\xi_0+\boldsymbol{r}_i,\xi_{obs}) - k_3\hat{\zeta}_i^T\nabla_{\xi_i} U_{att}(\hat{\xi}_i+\xi_0+\boldsymbol{r}_i,\xi_G) \\ - k_4\hat{\zeta}_i^T \sum_{s_j\in\overline{N}_i(t)} \nabla_{\xi_i} U_{rep}(\hat{\xi}_i,\hat{\xi}_j) + \hat{\zeta}_i^T k_1 \sum_{s_j\in N_i(t)} a_{ij}(t)[\hat{\xi}_j(t)-\hat{\xi}_i(t)] \\ - k_3\nabla_{\xi_i} U_{att}(\hat{\xi}_i+\xi_0+\boldsymbol{r}_i,\xi_G)]\end{aligned} \tag{21}$$

By simplifying (21), we can obtain that

$$\dot{V} = \sum_{i=1}^{n}[-\hat{\zeta}_i^T\hat{\xi}_i] \tag{22}$$

From (22), we can know that $\dot{V} \leq 0$. According to Lyapunov's second method for stability, the system described by (19) is asymptotically. Considering a set $\Omega = \{(\hat{\xi}_{ij},\hat{\zeta}_i)|V(t) \leq V_0\}$, where $\hat{\xi}_{ij} = \hat{\xi}_i - \hat{\xi}_j$ is bounded and $\hat{\zeta}_i^T\hat{\zeta}_i \leq \sum_{i=1}^{n}\hat{\zeta}_i^T\hat{\zeta}_i \leq 2V \leq 2V_0$. Therefore, $\parallel \hat{\zeta} \parallel \leq \sqrt{2V_0}$, that means $\hat{\zeta}_i$ is bounded. Then we can obtain that Ω is a compact set. Based on LaSalle's principle in [10], if the initial solution of the system is in Ω, the trajectories will converge to the maximum invariant set in $\overline{\Omega} = \{(\hat{\xi}_{ij},\hat{\zeta}_i) \in \Omega|\dot{V} = 0\}$.

From (22), we can know that if $\dot{V} = 0$, then $\hat{\xi}_i = 0(i = 1,2,\cdots,n)$ and $\zeta_i(t) = v_0(t)$ in $\overline{\Omega}$. Noted that $\frac{d(\hat{\xi}_i(t))}{dt}$, then $\hat{\xi}_i(t) \equiv c$. Therefore $\hat{\xi}_i - \hat{\xi}_j = 0$, that is $\xi_j - \xi_i = \boldsymbol{r}_{ij}$ and the desired formation is achieved under protocol (16).

Lemma 3 *: Considering a UAV system with n agents and the communication topology is jointly connected. Under protocol* (16)*, the desired formation is achieved with collision avoidance.*

Proof: Here, reduction to absurdity is used to prove that collision avoidance is realized between UAVs. Suppose UAV i and j collide at $t_1 > 0$ and their position states satisfy

$$\xi_i(t_1) = \xi_j(t_1), (i \neq j \ and \ i,j \in (1,2,\cdots,n)) \tag{23}$$

By (12), we can know

$$\frac{1}{2}\sum_{i=1}^{n} k_4[\sum_{s_j\in\overline{N}_i(t)} U_{rep}^{ij}(\hat{\xi}_i,\hat{\xi}_j)] = \frac{1}{2}\sum_{j=1}^{n} k_4[k \sum_{s_j\in\overline{N}_i(t)} 0.5k(\frac{1}{d(\xi_i,\xi_j)} - \frac{1}{d_{safe}})^2] \tag{24}$$

By (23) and(24), then

$$\lim_{t\to t_1}\frac{1}{2}\sum_{i=1}^{n}k_4[\sum_{s_j\in\overline{N}_i(t)}U_{rep}^{ij}(\hat{\xi}_i,\hat{\xi}_j)]=+\infty \tag{25}$$

However, by (20), we can know

$$\begin{aligned}\frac{1}{2}\sum_{i=1}^{n}k_4[\sum_{s_j\in\overline{N}_i(t)}U_{rep}^{ij}(\hat{\xi}_i,\hat{\xi}_j)] &= V-\sum_{i=1}^{n}[k_2\sum_{obs=1}^{l}U_{rep}^{i}(\hat{\xi}_i+\xi_0+\boldsymbol{r}_i,\xi_{obs})-\frac{1}{2}\hat{\zeta}_i^T\hat{\zeta}_i\\ &\quad-\frac{1}{4}\sum_{s_j\in\overline{N}_i(t)}a_{ij}(t)(\hat{\xi}_i-\hat{\xi}_j)^2-k_3U_{att}^{i}(\hat{\xi}_i+\xi_0+\boldsymbol{r}_i,\xi_G)]\\ &\leq V\leq V_0\end{aligned} \tag{26}$$

That is

$$\lim_{t\to t_1}\frac{1}{2}\sum_{i=1}^{n}k_4[\sum_{s_j\in\overline{N}_i(t)}U_{rep}^{ij}(\hat{\xi}_i,\hat{\xi}_j)]\leq V_0 \tag{27}$$

Clearly, (25) and (26) is contradictory. We can obtain that the collision avoidance is achieved during the flight. Also, the obstacle avoidance can be proved with the same method. In order to save space, the proof process is omitted here.

Remark 3: Based on the results, we can obtain that the formation can be achieved with collision/obstacle avoidance under the designed control protocol (16). It should be point out that the total energy V_t of UAV system is a finite value and it will change constantly during the flight in practice.

4 SIMULATIONS

In this section, two cases are provided to demonstrate the approach presented in this paper. A practical example adopted in [22] is considered. Different from the consensus protocol presented in [22], an improved protocol with collision/obstacle avoidance is designed. For simplicity, it is assumed that the elements of weighted adjacency matrix are 0 or 1, and all UAVs move in XY plane.

Case 1: Consider a system with five UAVs in an obstacle-free environment. Their desired formation structure of regular pentagon and undirected interaction topology are shown in Fig. 3, respectively.

The initial conditions of UAVs are given by Table 1

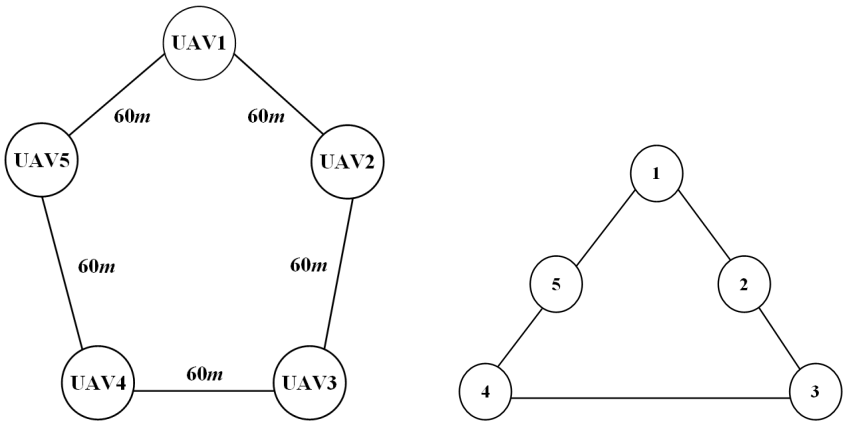

(a) The desired formation structure (b) The undirected interaction topology

Fig. 3: The desired formation structur and undirected interaction topology

Table 1: Initial states of all UAVs

UAV	x_i (m)	y_i (m)	v_{xi} (m/s)	v_{yi} (m/s)
UAV1	-0.15	0.02	-0.08	-0.02
UAV2	-12.25	-0.06	6.35	-0.06
UAV3	-12.25	-0.24	-0.08	-0.01
UAV4	-12.17	0.05	-4.46	-0.02
UAV5	-4.71	-0.08	-7.1	0.04

Table 2: Initial states of the system

UAV	x_i (m)	y_i (m)	v_{xi} (m/s)	v_{yi} (m/s)
UAV1	0	0	5	0
UAV2	60	5	0	3
UAV3	30	50	2	2
UAV4	130	120	0	0
UAV5	90	80	0	0

The parameters of control protocol (20) are given by $k_1 = 7.5, k_2 = 0, k_3 = 2.5, k_4 = 1.0$. The dynamic constraint of velocity is given by $v_0 \in [0, 15]$, and the safe distance of UAVs is 10 m. The gain coefficient of attractive potential field and repulsive potential field are chosen as $\varepsilon = 0.03$ and $\eta = 10.2$, respectively. Fig. 4. (a) shows the formation trajectories in simulation within 300s, where the initial states of UAVs are denoted by circles. We can see from the figure that all UAVs move along a circle, and at $time = 100s$, the formation structure of regular pentagon is achieved and maintained with five UAVs. Fig. 4. (b) shows the velocity of all UAVs. We can see that when the formation is achieved, the velocities of UAVs are identical. Compared with [22], the presented control protocol (20) has a better consistency. Fig. 5. (a) and Fig. 5. (b) show the velocity and position trajectorie errors between UAVs and desired formation. It is clearly that the velocity error and position error converge to zero finally.

Case 2: Consider a UAV system with one leader UAV1 and three followers in an environment with obstacles. Their desired formation structure of square and undirected interaction topology are shown in Fig. 6, respectively.

The initial conditions of the system are given by Table 2

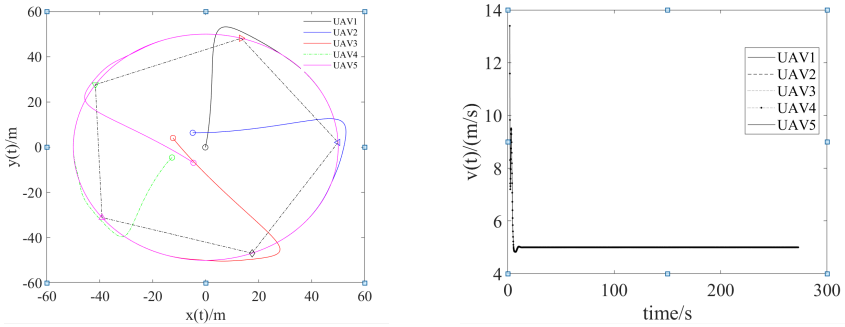

(a) Position trajectories of five UAVs (b) Velocity trajectories of five UAVs

Fig. 4: Position trajectories and velocity trajectories of five UAVs in case 1

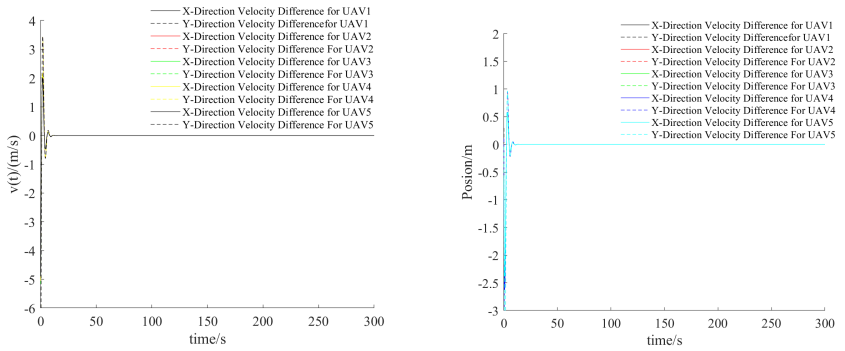

(a) Velocity trajectories errors (b) Position trajectories errors

Fig. 5: Position trajectories and velocity trajectories of five UAVs in case 1

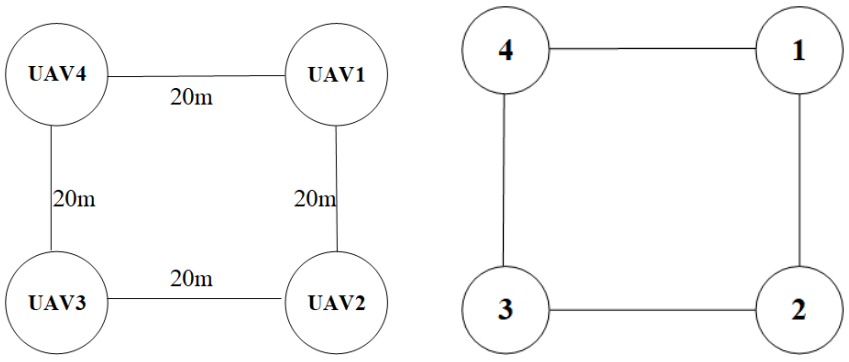

(a) The desired formation structure (b) The undirected interaction topology

Fig. 6: The desired formation structure and the undirected interaction topology

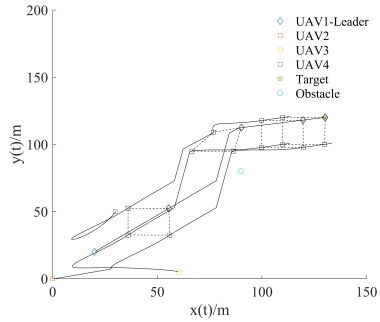

Fig. 7: The trajectories of five UAVs in case 2

The parameters of control protocol (20) is given by $k_1 = 7.6, k_3 = 2.0, k_2 = 0, k_4 = 1.0$. When the obstacle is detected by UAV, $k_2 = 18$, else $k_2 = 0$. The dynamic constraint of velocity is given by $v_0 \in [0, 15]$, and the safe distance of UAVs is $10m$. The gain coefficient of attractive potential field and repulsive potential field are chosen as $\varepsilon = 0.03$ and $\eta = 10.2$, respectively.

Fig. 7 shows the position trajectories of four UAVs during the flight with obstacle/collision avoidance. UAV1-leader is denoted by diamond, and others are denoted by square, respectively. Obstacle and target are denoted by circle and pentagram, respectively. First, the formation is achieved quickly and maintained if obstacle is not detected by UAVs. If obstacle is detected by any UAV or the distance between UAV i and UAV j is less than $10m$, the formation will take obstacle/collision avoidance first. After obstacle/collision avoidance, the formation will be achieved again. Different from [22], the initial states can be chosen randomly and collision will not occur under control protocol (20). Compared with [29], the improved potential field method with velocity constraint is designed so that attractive force and repulsive force can avoid falling into local minimum. The simulation results prove the control protocol (20) has a wider application.

5 CONCLUSION

In this paper, the leader-follower formation control problem of unmanned air vehicles(UAVs) flying with velocity constraint in an obstacle-laden environment has been studied. The linear control protocol is designed to achieve formation with obstacle/collision avoidance. The stability conditions of the consensus algorithm is analyzed by using a Lyapunov theory and LaSalle's principle. Finally, two applications have been given to show that the presented control protocol is validated and effective for formation flying with obstacle/collision avoidance and velocity constraint.

Future work will include realizing obstacle/collision avoidance in 3-D plane with time delay, and the directed communication topology graph will be taken into consideration.

References

1. R. Olfati-Saber, J. A. Fax and R. M. Murray, "Consensus and Cooperation in Networked Multi-Agent Systems," in Proceedings of the IEEE, vol. 95, no. 1, pp. 215-233, 2007.
2. Lifeng Ma, Zidong Wang, Qing-Long Han, "Consensus control of stochastic multi-agent systems: a survey", Science China Information Sciences, Volume 60, no. 12, pp. 1 ,2017
3. J. A. Fax, R. M. Murray, "Information flow and cooperative control of vehicle formations," IEEE Trans. Autom. Control, vol. 49, no. 9,pp. 1465–1476, 2004
4. H. Chen and J. Fei, "UAV path planning based on particle swarm optimization with global best path competition," Int. J. Pattern Recognit. Artif. Intell, vol. 32, 2018
5. "Forest fire monitoring using multiple small UAVs," in Proc. ACC, pp. 3531–3535, 2005
6. J. Kim and J. P. Hespanha, "Cooperative radar jamming for groups of unmanned air vehicles," in Proc. CDC, pp. 632–637, 2004
7. A. Jadbabaie, J. Lin, A. S. Morse, "Coordination of groups of mobile autonomous agents using nearest neighbor rules," IEEE Trans. Autom. Control, vol. 48, no. 6, pp. 988–1001, 2003
8. R. Olfati-saber, "Flocking for multi-agent dynamics systems: Algorithms and theory," IEEE Trans. Autom. Control, vol. 51, no. 3, pp. 401–420, 2006
9. J. Wang, H. Wu, "Leader–following formation control of multi-agent systems under fixed and switching topologies", International Journal of Control,vol. 85, pp. 695–705, 2012
10. D. B. Edwards, T. A. Bean, D. L. Odell, and M. J. Anderson, "Leader-follower algorithm for multiple AUV formations", Proc. IEEE/OES Auton. Underwater Vehicles, pp. 40–46, 2004,
11. T. Balch, R.C. Arkin, "Behavior-based formation control for multi-robot teams", IEEE Transactions on Robotics and Automation, vol. 14, pp. 1–15, 1998
12. A. Brunete, M. Hernando, E. Gambao, J.E. Torres, "A behaviour-based control architecture for heterogeneous modular, multi-configurable, chained microrobots", Robotics and Autonomous Systems, vol. 60, pp. 1607–1624, 2012
13. A. Seuret, D. V. Dimarogonas, and K. H. Johansson, "Consensus under communication delay," Proc. 47th IEEE Conf. Decision Control, pp. 4922–4927, 2008
14. Y.-P. Tian, C.-L. Liu, "Consensus of multi-agent systems with diverse input and communication delays," IEEE Trans. Autom. Control, vol. 53, no. 9, pp. 2122–2128, 2008
15. H. M. Guzey, T. Dierks, S.JagannathanL, Acar, "Modified Consensus-based Output Feedback Control of Quadrotor UAV Formations Using Neural Networks", Journal of Intelligent & Robotic Systems, Volume 94, Issue 1, pp 283–300, 2019.
16. W. Ren, "Consensus strategies for cooperative control of vehicle formations," IET Control Theory Appl, vol. 1, no. 2, pp. 505–512, 2007
17. Lawton J R, Beard R W, "Synchronized Multiple Spacecraft Rotations", Automatica, vol. 38, no. 8, pp. 1359-1364, 2002
18. BausoD, GiarreL, Pesenii R, "Attitude Alignment of a Team of UAVs under Decentralized Information Structure", IEEE Conference on Control Applications, pp. 486-491, 2003
19. Li, Z., Wen, G., Duan, Z., Ren, W, "Designing fully distributed consensus protocols for linear multi-agent systems with directed graphs". IEEE Transactions on Automatic Control, vol. 60, no. 4, pp. 1152–1157, 2015.
20. Tao Feng, Weiping Fan, Jiuyang Tang,Weixin Zeng, "Consensus-based Robust Clustering and Leader Election Algorithm for homogeneous UAV clusters", Journal of Physics: Conference Series, Volume 93, no. 1–2, pp 213–226, 2019.
21. Ren, W., and Beard, R.W.: 'Consensus seeking in multiagent systems under dynamically changing interaction topologies', IEEE Trans. Autom. Control, vol. 50, no. 5, pp. 655–661, 2005

22. X. Dong, B. Yu, Z. Shi, Y. Zhong, "Time-Varying Formation Control for Unmanned Aerial Vehicles: Theories and Applications," in IEEE Transactions on Control Systems Technology, vol. 23, no. 1, pp. 340-348, 2015.
23. Tanner, H.G., Jadbabaie, A., and Pappas, G.J.: 'Stable flocking of mobile agents, Part i: fixed topology'. Proc. IEEE Conf. on Decision and Control, pp. 2010–2015, 2003
24. Y. Kuriki and T. Namerikawa, "Formation Control of UAVs with a Fourth-order Flight Dynamics," Decision and Control (CDC), IEEE 52nd Annual Conference, pp. 6706-6711, 2013
25. R. Olfati-Saber and R. M. Murray, "Consensus problems in networks of agents with switching topology and time-delays," IEEE Trans. Autom. Control, vol. 49, no. 9, pp. 1520–1533, 2004.
26. X. Wang, V. Yadav and S. N. Balakrishnan, "Cooperative UAV Formation Flying With Obstacle/Collision Avoidance," in IEEE Transactions on Control Systems Technology, vol. 15, no. 4, pp. 672-679, 2007.
27. Yasuhiro Kuriki, Toru Namerikawa, "Consensus-based Cooperative Formation Control with Collision Avoidance for a Multi-UAV System",2014 American Control Conference (ACC), 2014.
28. Hassan K. Khalil, Nonlinear Systems, Prentice Hall, 2001
29. Y. Koren and J. Borenstein, "Potential field methods and their inherent limitations for mobile robot navigation," Proceedings. 1991 IEEE International Conference on Robotics and Automation, vol.2, pp. 1398-1404, 1991
30. Xiao Yu, Lu Liu, Senior Member, IEEE, "Distributed Formation Control of Nonholonomic Vehicles Subject to Velocity Constraints", IEEE Trans, Industrial Electronisc, vol. 63, no.2, 2016